3D Dynamic RTN Simulation of a 25nm MOSFET: The Importance of Variability in Reliability Evaluation of Decananometer Devices

S. M. Amoroso*, F. Adamu-Lema*, S. Markov*, L. Gerrer* and A. Asenov*,+
* Device Modelling Group, University of Glasgow, e-mail: salvatore.amoroso@glasgow.ac.uk
+ Gold Standard Simulations Ltd, Glasgow G12 8QQ, Scotland, UK

Introduction: Random telegraph noise (RTN) is a rapidly increasing threat to advanced CMOS scaling [1-2]. The impact of RTN on the reliability of SRAM memory cell operation has been shown to be important starting from the 40 nm generation [3] and to be increasing with cell scaling [4-5]. A robust design aiming to RTN threshold voltage instabilities suppression should rely on accurate understanding of the physics governing the RTN phenomenon, including also the effects of variability induced by the atomistic nature of dopants [6-7]. Further, the RTN instabilities exhibit significant transient effects when the device is biased under time-dependent gate voltages [8]. In this case, evaluating the reliability by means of a steady-state analysis can lead to misleading results [9]. In this work we present, for the first time, a dynamic RTN simulation study employing a physics-based trapping/detrapping model in presence of atomistic doping. Our analysis shows that variability induced by atomistic doping plays an important role in determining the reliability features of nanoscale devices, both in transient and steady-state conditions. These results advocate the use of 3D statistical simulations as fundamental complement of any experimental characterization of oxide traps leading to RTN.

Simulation methodology: We performed 3D simulations of a well-scaled 25 nm MOSFET device using the GSS 'atomistic' simulator GARAND featuring a drift-diffusion approximation with density gradient quantum corrections [10]. Fig.1 shows the effective potential in the presence of a random configuration of dopants. The single oxide trap leading to RTN is modelled by assigning three positional coordinates (x_T,y_T,z_T), one energy level ($E_{T,0}$) and a capture cross-section (σ). In the present study we evaluate the impact of the trap position variability (x_T,y_T) over the channel area, keeping constant z_T=0.3nm (from Si/SiO_2 interface), $\sigma=10^{-14}$ cm^2, $E_{T,0}$=3.33eV (below the SiO_2 conduction band).

Simulation of RTN signal is achieved within a Kinetic Monte Carlo (KMC) loop, as shown in Fig.2. After solving the 3D electrostatics and current continuity equation (at V_G=0.15V,V_D=0.05V), the average capture time $<\tau_c>$ for the single trap is computed integrating the tunnelling gate current density that reaches the trap (WKB approximation) over an area equal to the trap cross-section σ [11]. The average emission time $<\tau_e>$ is calculated according to eq. (1) based on SRH statistics (Fig.3). Then the actual capture and emission constants are randomly extracted from exponential distributions of average value $<\tau_c>$ and $<\tau_e>$. Based on these constants, a KMC-engine choose the next event (capture or emission) and the dynamic simulation time is increased by the extracted τ_c or τ_e. The loop is repeated until the desired reading time is reached. An example of simulated dynamic drain current in presence of a single active RTN trap is presented in Fig.4.

Reliability results in presence of variability: Figs. 5 and 6 show the dynamic trap occupancy for the two cases studied – continuously doped device and atomistically doped device.

In both cases the occupancy of the single trap is evaluated for two different trap positions (POS 1 and POS 2 in Fig.7) over the channel area. The trap occupancy, defined as in [9], is obtained by averaging more than 200 dynamic RTN simulations (as Fig. 4) for each case. In the same figures the analytical result obtained from Eqs. (2)-(4), where $<\tau_c>$ and $<\tau_e>$ are established from the 3D statistical simulations, is also shown. Note that eqs. (2)-(4) are easily derived assuming that RTN can be described as a Markovian chain, which has been experimentally and analytically demonstrated [12]. Figs. 5 and 6 clearly show the transient effect on the RTN trap occupancy. In particular, erroneous results of reliability performance are obtained for devices operating under dynamic condition with frequency $f > 1/\tau^*$, if trap occupancy is evaluated using a steady-state analysis. Besides, comparison of Fig.5 and Fig.6 demonstrates the critical role played by variability on reliability performance. Indeed, Fig. 6 shows that the RTN behaviour, in both transient and steady-state regime, dramatically changes depending on the trap position over the channel active area. Fig. 5 highlights that only a small part of this variability can be attributed to the 3D non-uniform electrostatics over the channel area of a nanoscale transistor. Tab.1 reports the RTN proprieties of the two simulated cases. Finally, we show in Fig.8 the variability of $<\tau_c>$ and $<\tau_e>$ due to change of (x_T,y_T) over the whole channel area, emphasizing the impact of the atomistic doping on RTN time constants.

Conclusions: We have presented for the first time a 3D dynamic simulation analysis for the reliability evaluation of a decananometer MOSFET device. We have shown that variability due to atomistic doping is of outmost importance in assessing the reliability performance of nanoscale devices, in both transient and steady-state operating regimes.

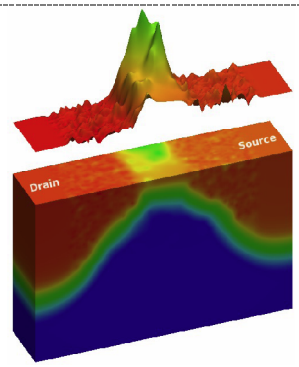

Fig.1 Effective potential for the 25nm atomistic MOSFET (V_G=0.15V,V_D=0.05V).

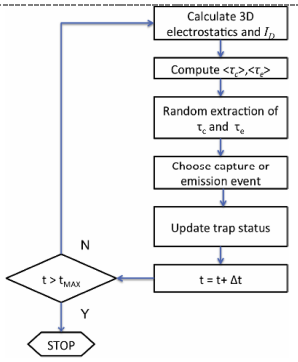

Fig.2 Kinetic MonteCarlo loop for dynamic RTN simulation.

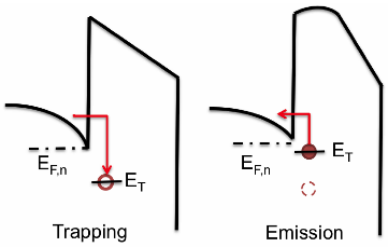

Fig.3 Schematics of the conduction band diagram illustrating trapping and emission process.

$$\frac{\langle \tau_e \rangle}{\langle \tau_c \rangle} = \exp\left(-\frac{E_T - E_{F,n}}{kT}\right) \quad (1)$$

$$Occ_{in}(t) = Occ_{ss}\left|1 - \exp(-t/\tau^*)\right| \quad (2)$$

$$Occ_{ss} = \frac{\langle \tau_e \rangle}{\langle \tau_e \rangle + \langle \tau_c \rangle} \quad (3)$$

$$\tau^* = \frac{\langle \tau_e \rangle \langle \tau_c \rangle}{\langle \tau_e \rangle + \langle \tau_c \rangle} \quad (4)$$

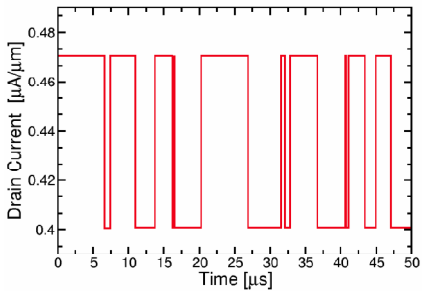

Fig.4 Example of simulated dynamic drain current in presence of a single active RTN trap in the gate oxide.

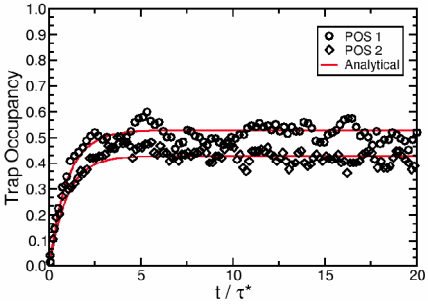

Fig.5 Trap occupancy versus normalized simulation time for the *continuously* doped device in Fig.7 (normalization factors τ * are given in Tab.1)

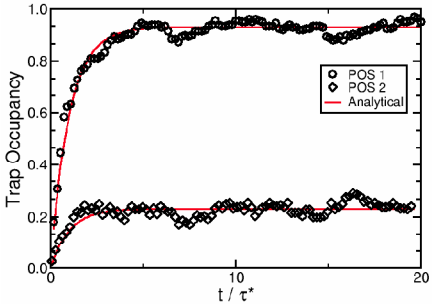

Fig.6 Trap occupancy versus normalized simulation time for the *atomistic* device in Fig.7 (the values of the normalization factor τ* are given in tab.1)

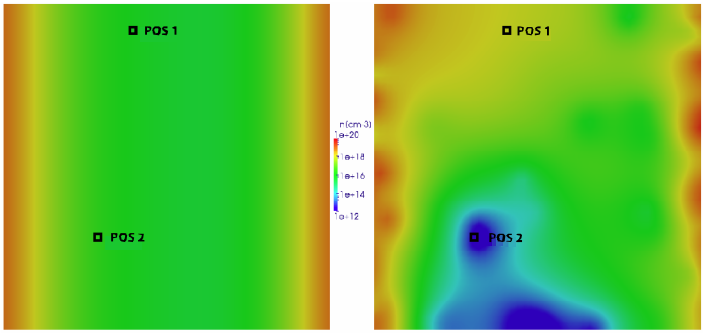

Fig.7 Electron density in the cannel active area for a *continuously* doped device (left) and an *atomistic* device (right). The two projected positions (x_T,y_T) of the analysed trap are also indicated. Traps sketched in figure are unoccupied.

	τ_c	τ_e	τ*	OCC_{ss}
CONT.				
POS 1	2.6e-6	2.9e-6	1.4e-6	52%
POS 2	4.1e-6	3.2e-6	1.8e-6	43%
ATOM.				
POS 1	5.9e-8	8.2e-7	5.5e-8	93%
POS 2	6.5e-2	2.0e-2	1.5e-2	23%

Tab.1 Computed τ_c, τ_e, τ* and stationary occupancy for the two positions indicated in Fig.7, for the case of *continuously* doped device and *atomistic* device.

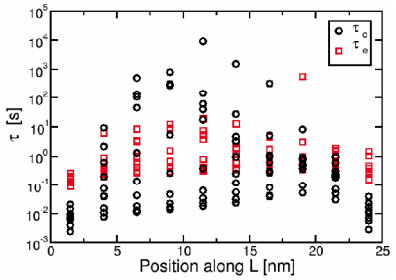

Fig.8 Simulated <τ_c> and <τ_e> as a function of trap position along L for 100 traps uniformly distributed over the channel area (atomistic device in Fig.7).

References

[1] T. Nagumo *et al.*, IEDM 2010, pp.628-631
[2] J.P. Campbell *et al.*, IRPS 2009, pp.382-388
[3] K. Takeuchi *et al.*, VLSI 2010, pp.189-190
[4] N. Tega *et al.*, VLSI 2009, pp.50-51.
[5] A. Ghetti *et al.*, IEDM 2008, pp.1-4.
[6] A. Mauri *et al.*, IEDM 2011, pp.405-408.
[7] A. Asenov *et al.*, Trans.Elec.Dev. pp.839-845 (2003).
[8] B. Dierickx *et al.*, J.Appl.Phys., pp.2028-2029 (1992).
[9] J. S. Kolhatkar, IEDM 2004, pp.759-762.
[10] http://www.goldstandardsimulations.com
[11] S. M. Amoroso, IEDM 2010, pp.540-543.
[12] C. M. Compagnoni *et al.*, Trans.Elec.Dev. pp.388-395 (2008).